

Supporting Information

Multilayer NiO@Co₃O₄@Graphene Quantum Dots Hollow Spheres for High-Performance Lithium-Ion Batteries and Supercapacitors

Xiaojie Yin^{1,†} Chuanwei Zhi^{1,†} Weiwei Sun², Li-Ping Lv^{2*} and Yong Wang^{1*}

¹*School of Environmental and Chemical Engineering*

²*Institute of Green Chemical Engineering and Clean Energy*

Shanghai University, 99 Shangda Road, Shanghai, P. R. China, 200444

*Corresponding authors: Tel: +86-21-66137723/66138091

Email address: yongwang@shu.edu.cn; liping_lv@shu.edu.cn

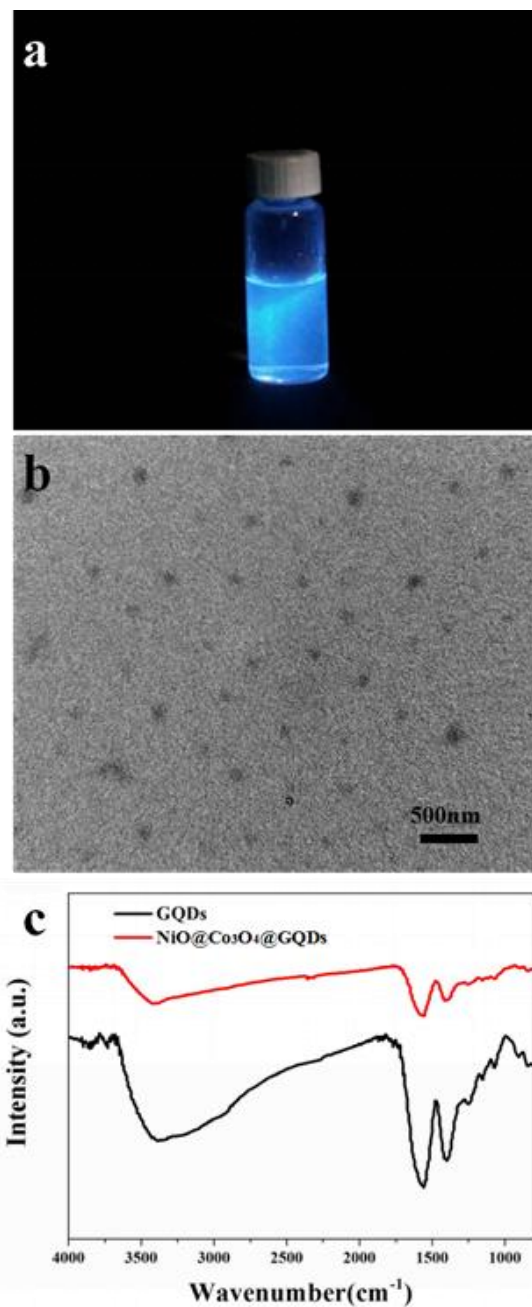


Figure S1. a) the digital photo of GQDs solution under UV light (365 nm). b) TEM image of GQDs. c) FTIR curves of GQDs and NiO@Co₃O₄@GQDs.

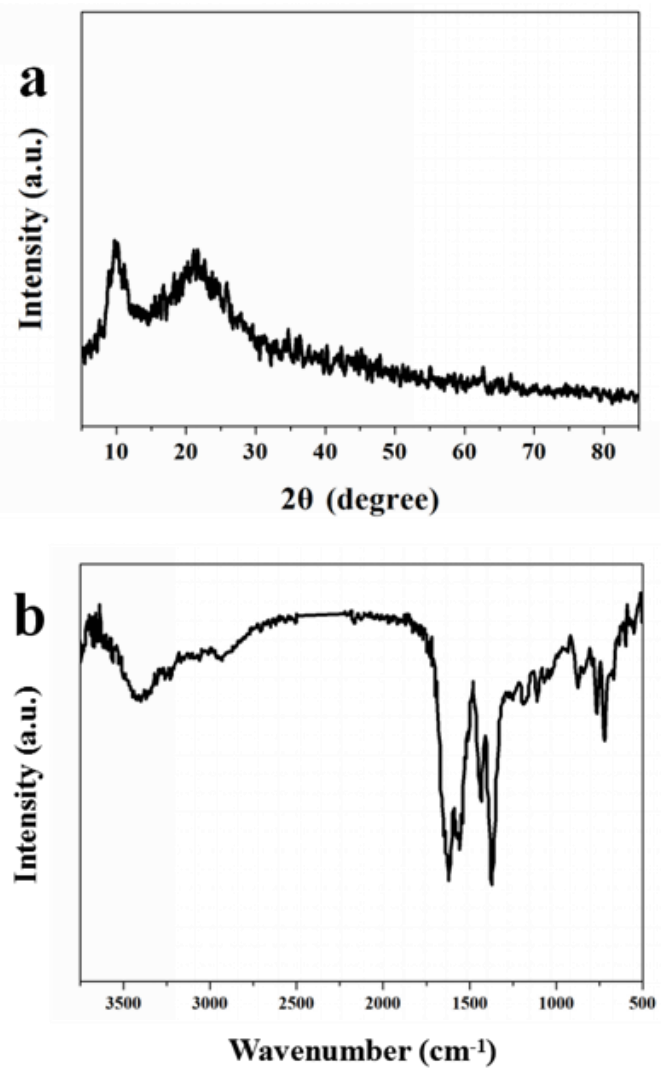


Figure S2. a) XRD and b) FTIR curves of Co-Ni-BTC MOF.

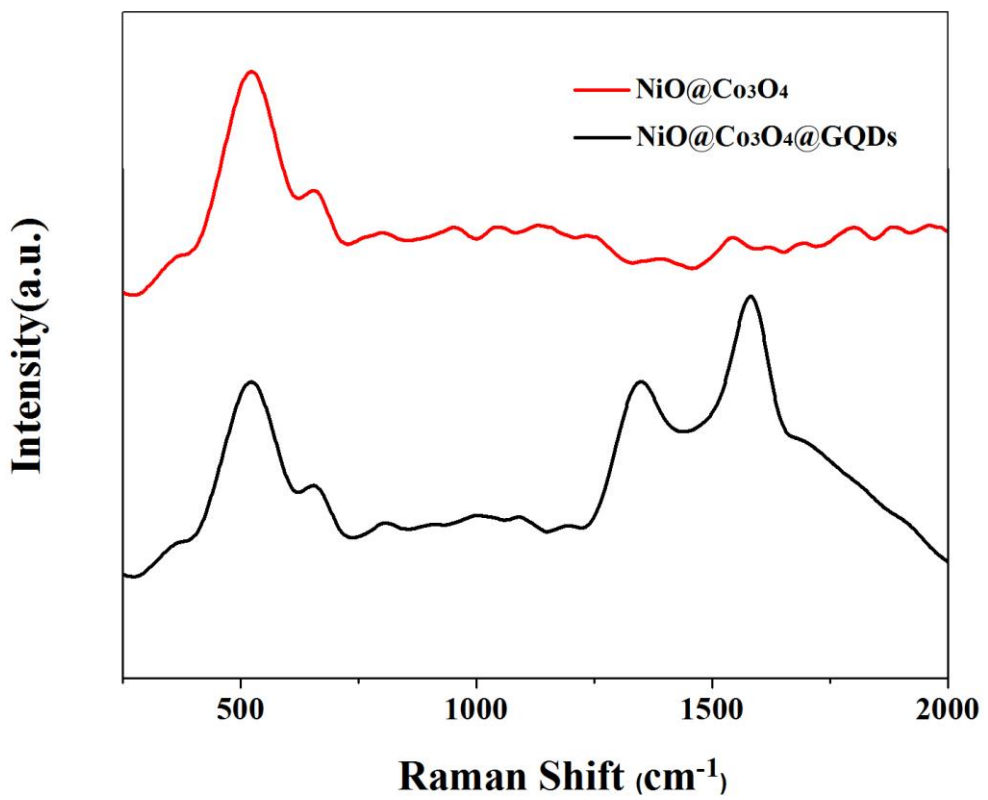


Figure S3. Raman spectra for NiO@Co₃O₄@GQDs and NiO@Co₃O₄.

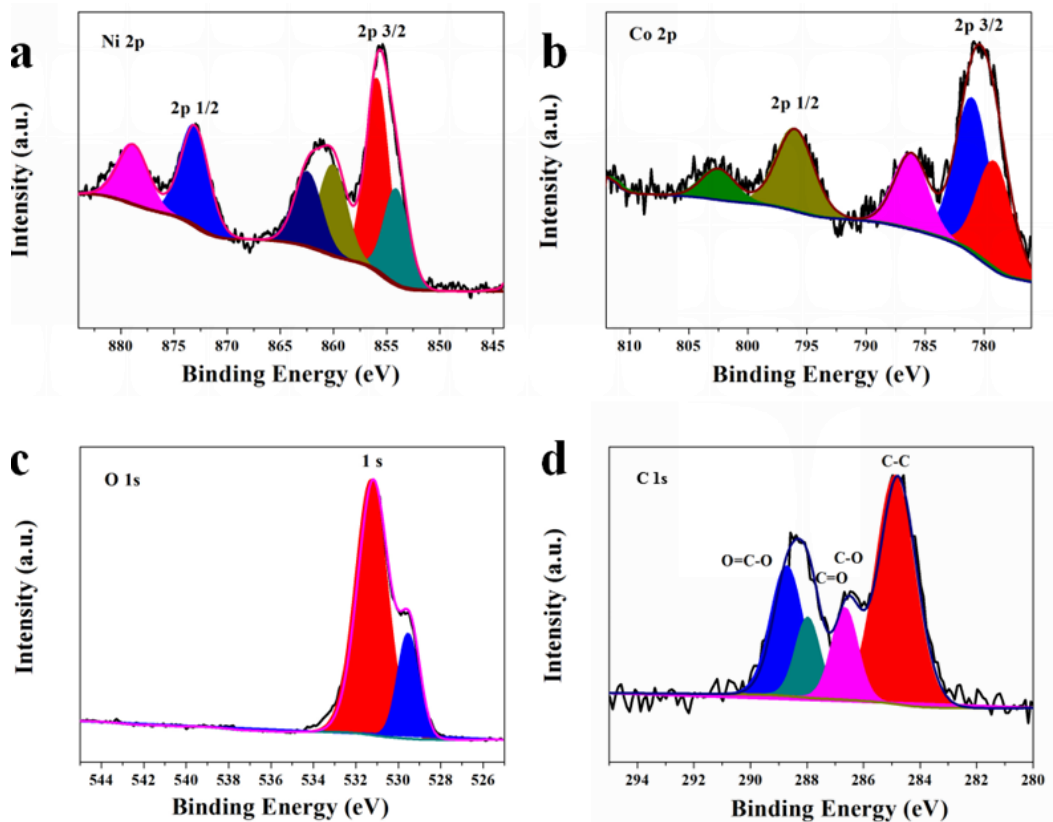


Figure S4. XPS spectra of NiO@Co₃O₄@GQDs: a) Ni 2p, b) Co 2p, c) O 1s and d) C 1s.

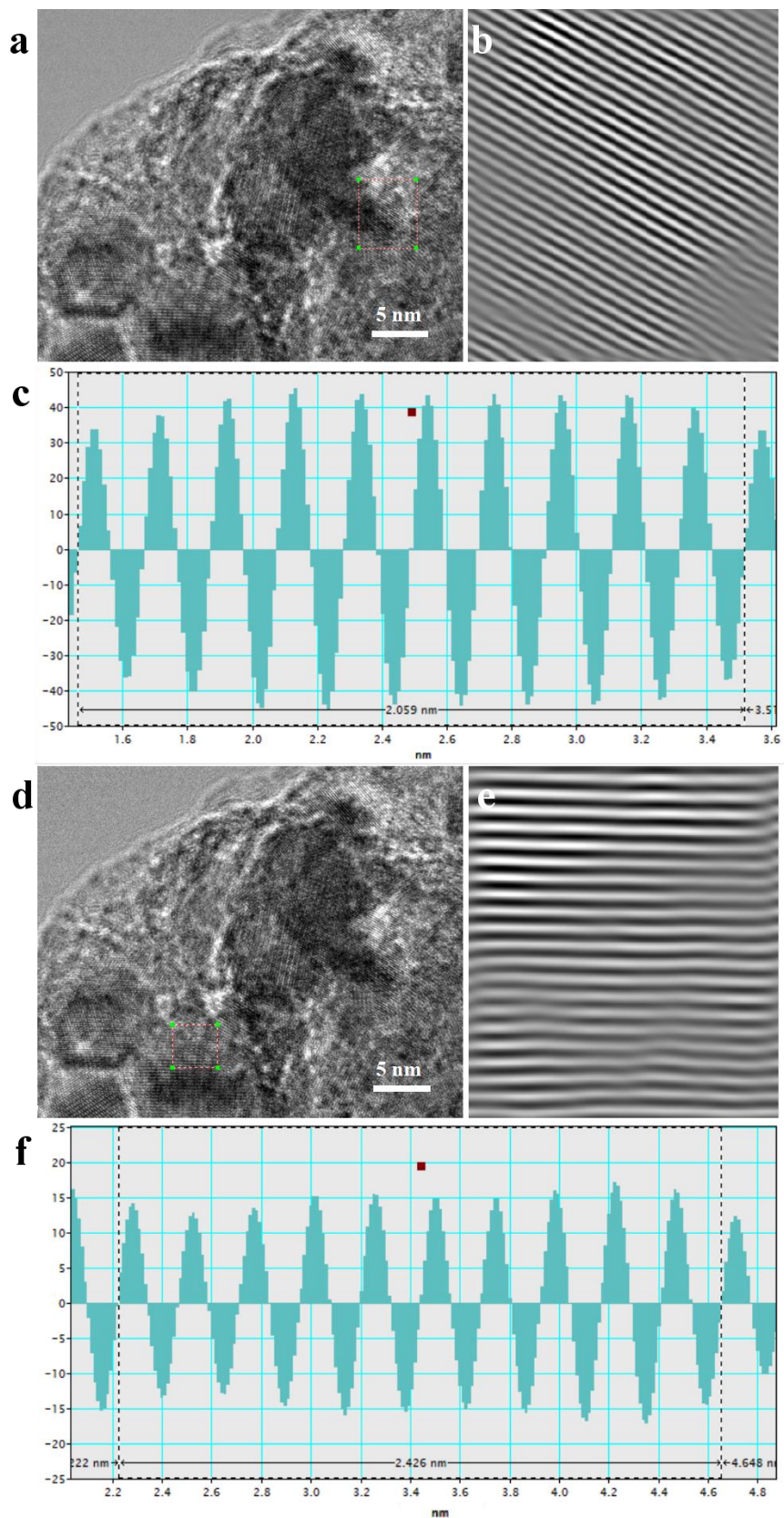


Figure S5. a, d) HRTEM images of NiO@Co₃O₄@GQDs. Lattice fringes of b) (100) plane of graphene and e) (111) plane of NiO. Images in c, f) indicate the lattice spacing of ten lattice fringes of the two phases, respectively.

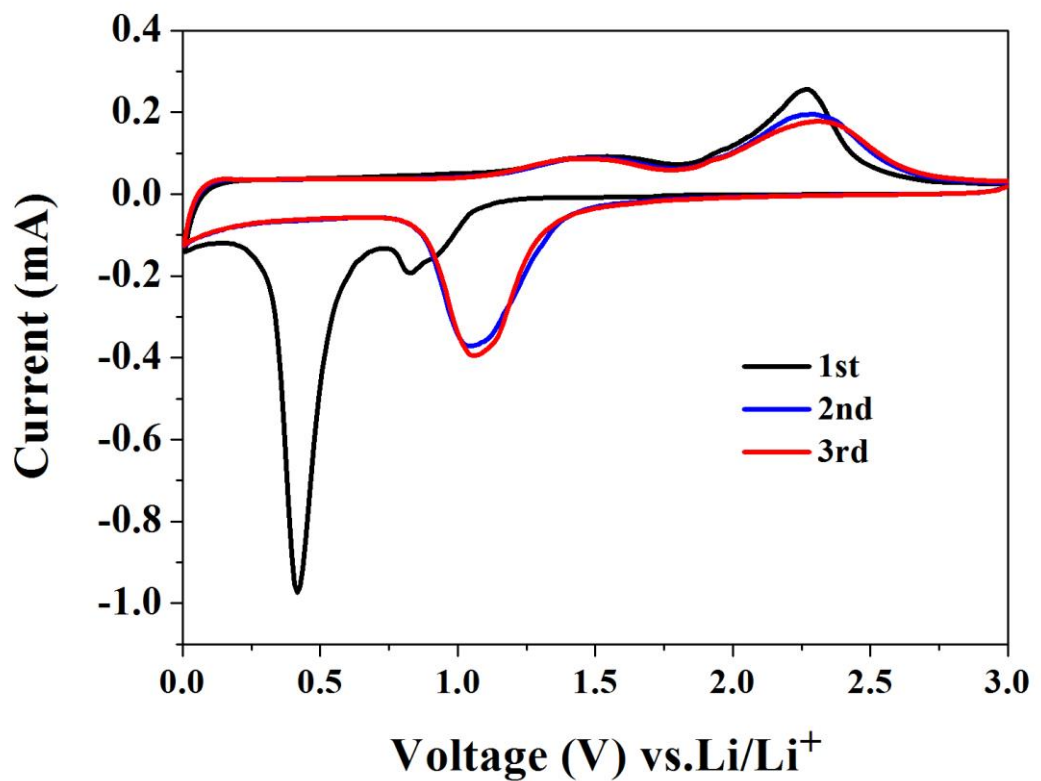


Figure S6. CV profiles of the first three cycles of NiO@Co₃O₄ at a scan rate of 0.1 mV s⁻¹.

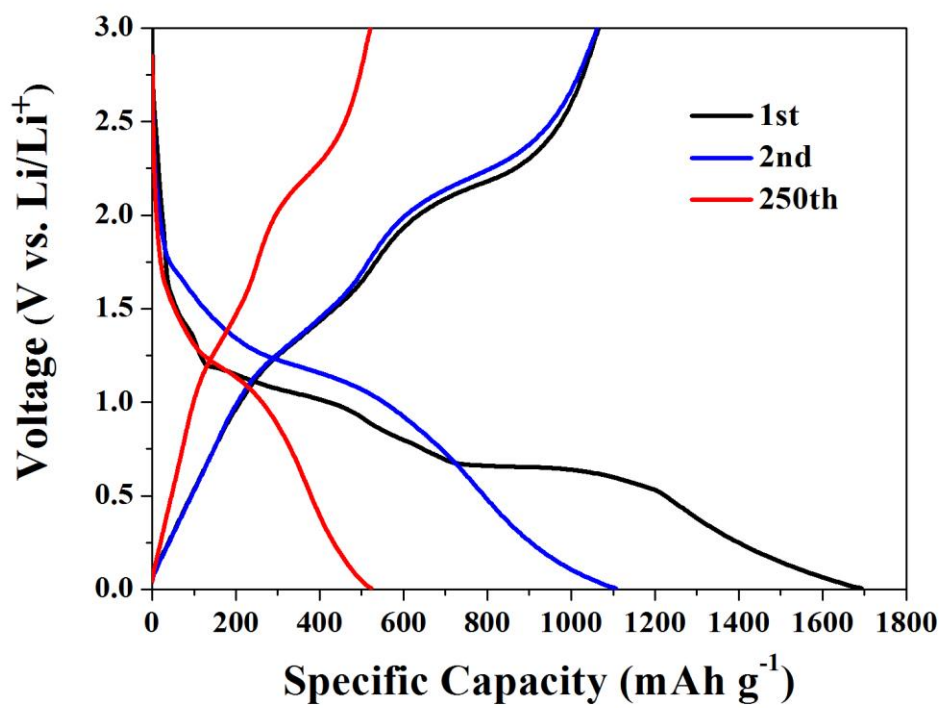


Figure S7. Discharging/charging profiles of 1st, 2nd and 250th cycle of NiO@Co₃O₄.

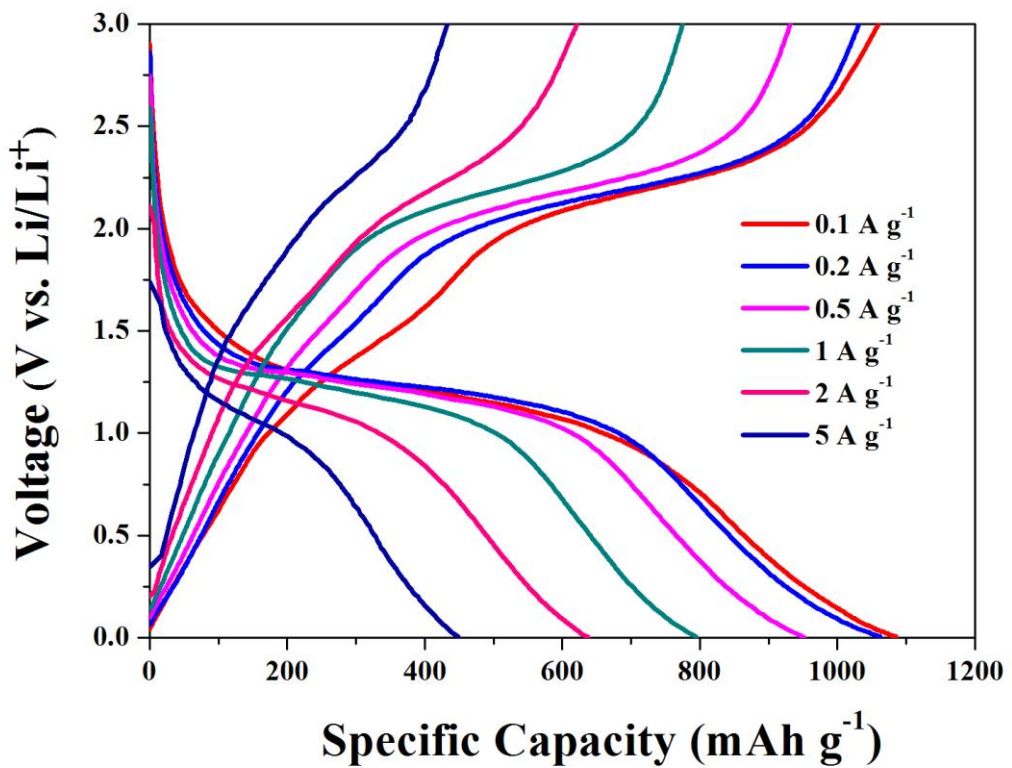


Figure S8. The voltage profile at different C-rates (0.1, 0.2, 0.5, 1, 2 and 5 A g⁻¹) of NiO@Co₃O₄@GQDs.

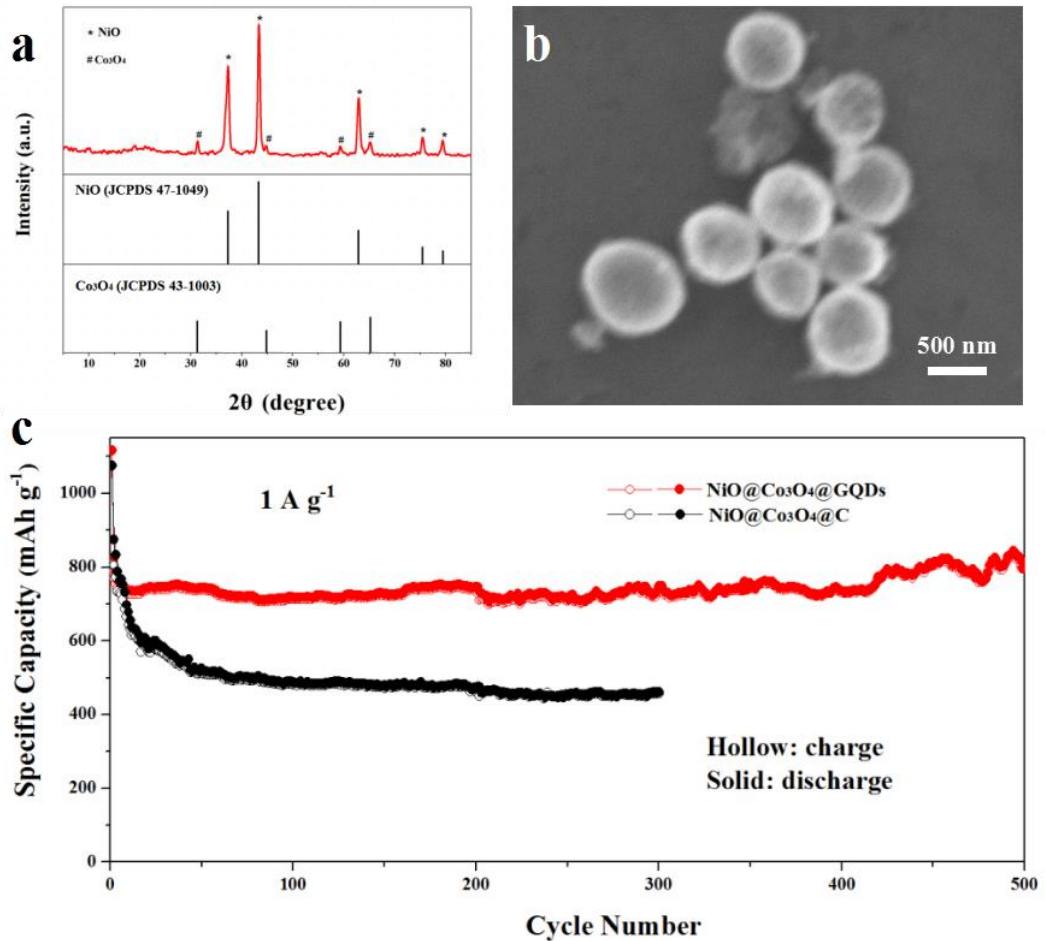


Figure S9. a) XRD patterns and b) SEM image of NiO@Co₃O₄@C. c) cycling performance of NiO@Co₃O₄@GQDs and NiO@Co₃O₄@C at 1 A g^{-1} .

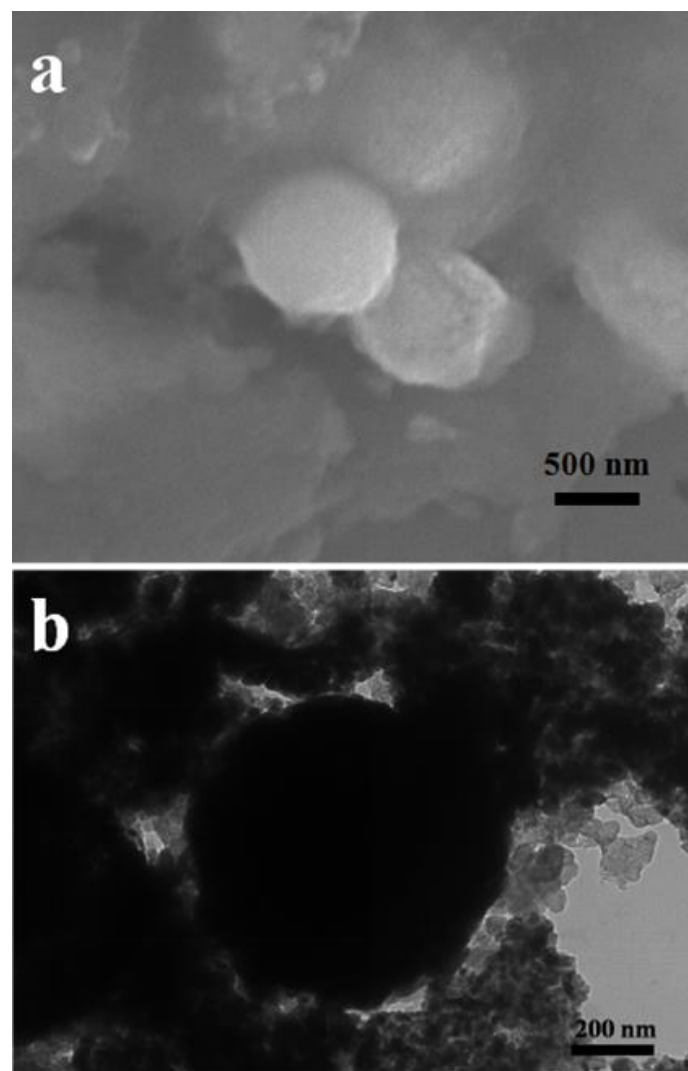


Figure S10. a) SEM and b) TEM image of NiO@Co₃O₄@GQDs anode for LIBs after 250 cycles.

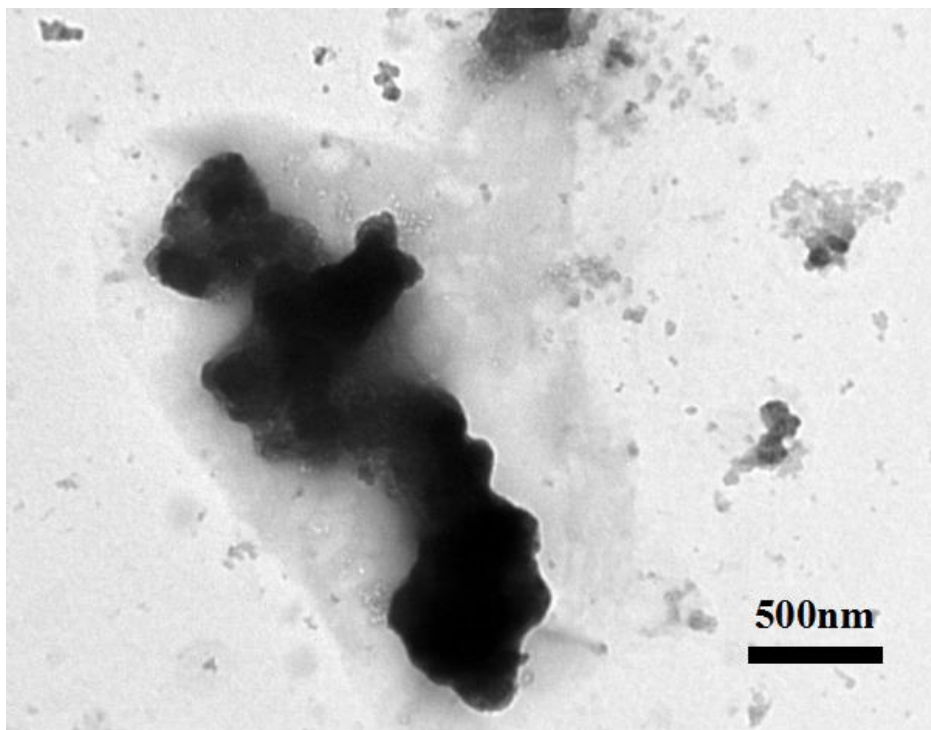


Figure S11. TEM image of NiO@Co₃O₄ anode for LIBs after 250 cycles.

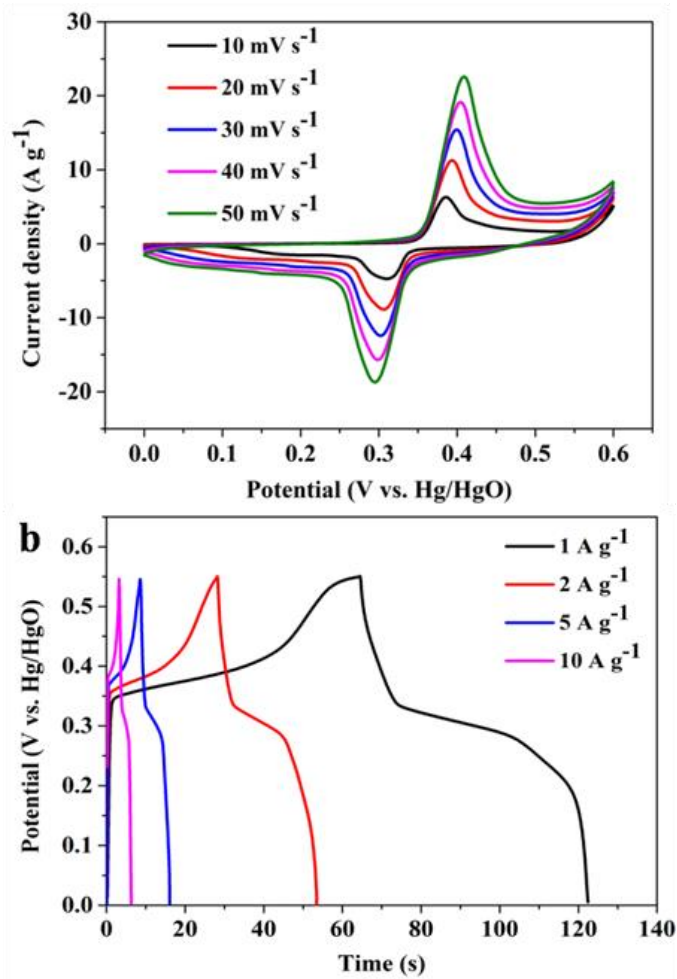


Figure S12. a) CV curves of the GQDs electrode at various scan rates. b) Galvanostatic charge-discharge curves of the GQDs electrode at different current densities.

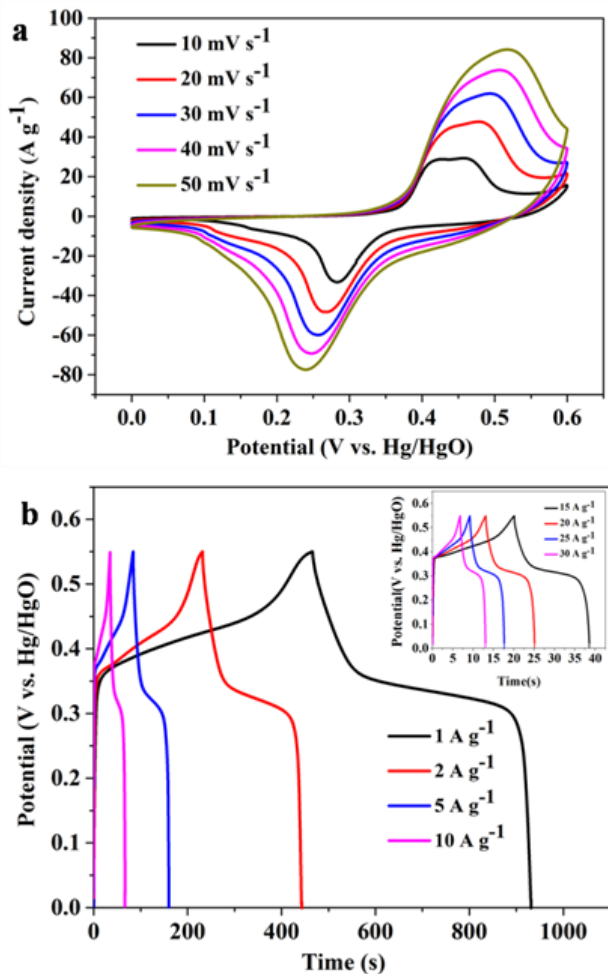


Figure S13. a) CV curves of the NiO@Co₃O₄ electrode at various scan rates. b) Galvanostatic charge-discharge curves of the NiO@Co₃O₄ electrode (1-10 A g^{-1} and 15-30 A g^{-1} , the inset).

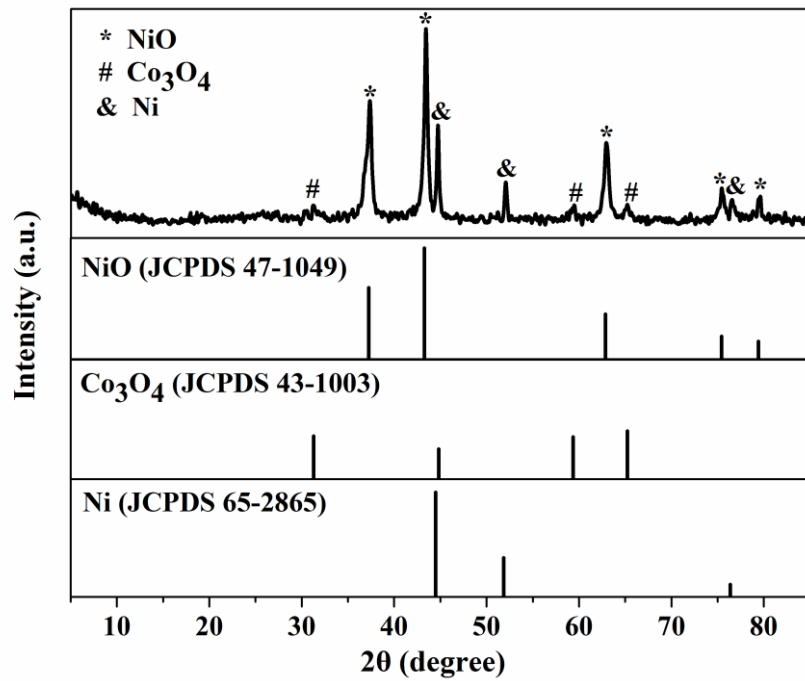


Figure S14. XRD data of NiO@Co₃O₄@GQDs after 3000 cycling tests of supercapacitor performance in three-electrode system.

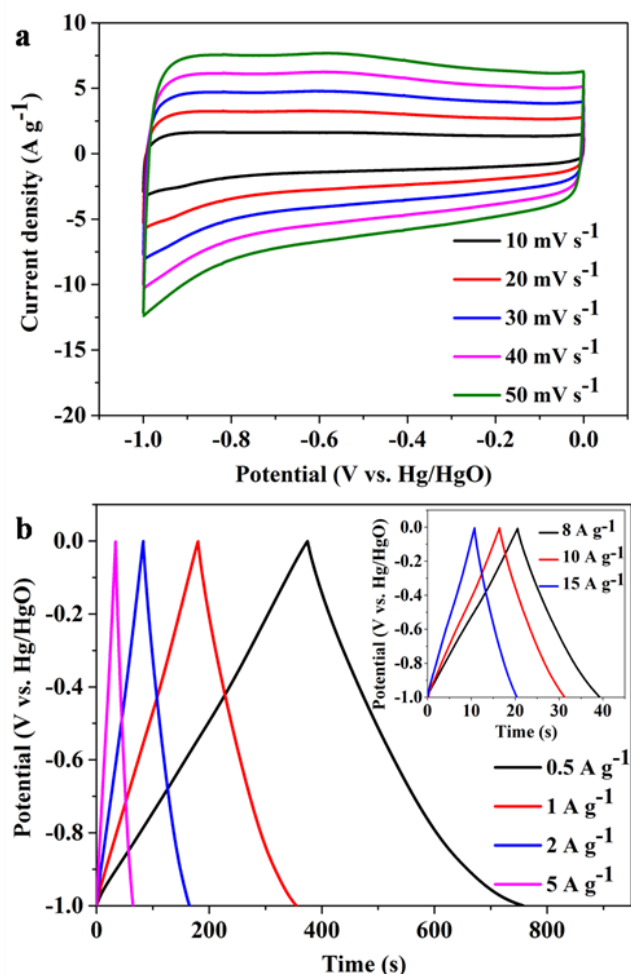


Figure S15. a) CV curves of the AC electrode at various scan rates. b) Galvanostatic charge-discharge curves of the AC electrode ($0.5\text{-}5 \text{ A g}^{-1}$ and $8\text{-}15 \text{ A g}^{-1}$, the inset).

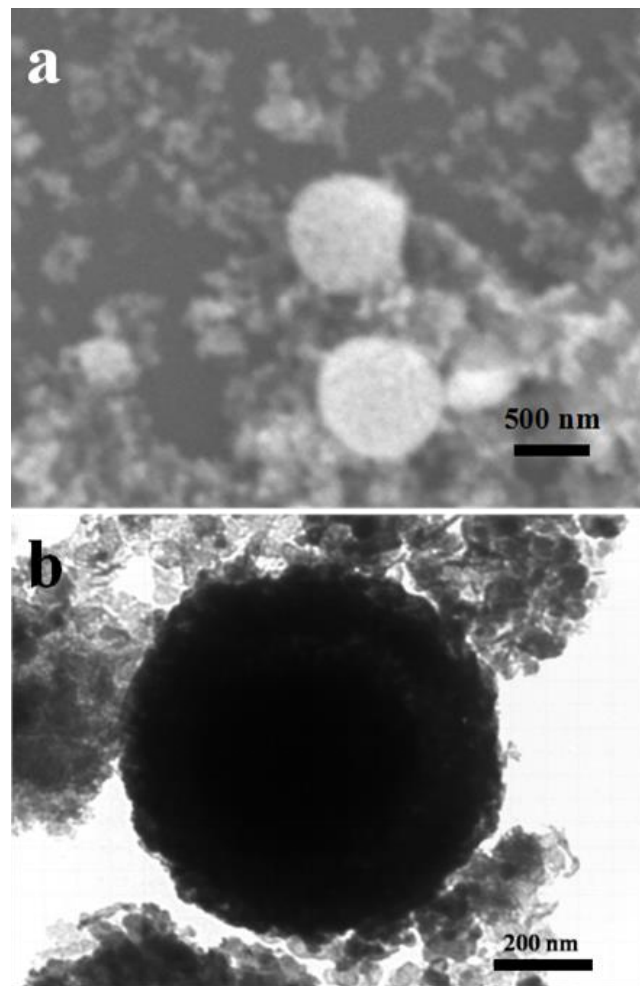


Figure S16. a) SEM and b) TEM image of the NiO@Co₃O₄@GQDs cathode for ASC device after 10000 cycles.

Table S1. The element analysis data of the NiO@Co₃O₄@GQDs composite.

| Samples | Elemental contents (wt%) | | |
|--|--------------------------|------|------|
| | C | N | H |
| NiO@Co ₃ O ₄ @GQDs | 15.12 | 0.04 | 1.15 |

Table S2. Electrochemical properties comparison of NiO@Co₃O₄@GQDs of this work and previous Co-Ni bimetal-oxide based anode for LIBs. (IRC: initial reversible capacity, mAh g⁻¹; RRC: retained reversible capacity, mAh g⁻¹; CN: cycle number; CD: current density, mA g⁻¹; V: voltage, V)

| Composite | Morphology | IRC | RRC/CN | CD | V | References |
|--|---------------------------------|--------|------------|-----|-----------|------------|
| NiO@Co ₃ O ₄ @GQDs | Multilayer | | | | | |
| | Hollow | ~ 1300 | ~ 1327/250 | 100 | 0.005-3.0 | This work |
| Ni _x Co _{3-x} O ₄ | Multi-shelled Hollow Sphere | ~ 1139 | ~ 1109/100 | 100 | 0.005-3.0 | 1 |
| | Multi-shelled Hollow Spheres | ~ 905 | ~ 706/100 | 200 | 0.01-3.0 | 2 |
| NiCo ₂ O ₄ | Nanosheet | 1015 | 988/50 | 200 | 0.01-3.0 | 3 |
| NiCo ₂ O ₄ | Microrods | 1046 | 857/100 | 100 | 0.01-3.0 | 4 |
| NiCo ₂ O ₄ | Nanocube | 1161 | 1058/200 | 100 | 0.01-3.0 | 5 |
| NiCo ₂ O ₄ | Nanorod | ~ 1095 | ~ 1000/400 | 500 | 0-3.0 | 6 |
| NiCo ₂ O ₄ /CNT | Nanoparticle | 1281 | ~ 1020/200 | 300 | 0-3.0 | 7 |
| NiCo ₂ O ₄ -C | Nanorod | ~ 1252 | ~ 1081/200 | 100 | 0.01-3.0 | 8 |
| NiO-CoO | Nanoneedles | 692 | 801/200 | 200 | 0.01-3.0 | 9 |
| NiO-Co ₃ O ₄ | Nanoplate | ~ 772 | 633/70 | 100 | 0.005-3.0 | 10 |
| NiCo-NiCoO ₂ /C | Nanoparticle | ~ 748 | 861/100 | 100 | 0.01-3.0 | 11 |
| CoO-NiO-C | Nanoflower | 731 | 562/60 | 100 | 0.002-3.0 | 12 |
| NiCoO ₂ /rGO/ NiCoO ₂ | Sandwich Nanosheets | 850 | 998/60 | 100 | 0.01-3.0 | 13 |
| Ni-Co-Mn-O | Multi-shelled Hollow Spheres | ~ 1470 | ~ 1097/250 | 200 | 0.01-3.0 | 14 |

References:

1. L. L. Wu, Z. Wang, Y. Long, J. Li, Y. Liu, Q. S. Wang, X. Wang, S. Y. Song, X. G. Liu, H. J. Zhang, Multishelled Ni_xCo_{3-x}O₄ Hollow Microspheres Derived from Bimetal-Organic Frameworks as Anode Materials for High-Performance Lithium-Ion Batteries. *Small* **2017**, 1604270.
2. L. F. Shen, L. Yu, X. Y. Yu, X. G. Zhang, X. W. Lou, Self-templated formation of uniform NiCo₂O₄ hollow spheres with complex interior structures for lithium-ion batteries and supercapacitors. *Angew. Chem. Int. Ed.* **2015**, 54, 1868-1872.
3. Z. Y. Fan, B. R. Wang, Y. X. Xi, X. Xu, M. Y. Li, J. Li, P. Coxon, S. D. Cheng, G. X. Gao, C. H. Xiao, G. Yang, K. Xi, S. J. Ding, R. V. Kumar, A NiCo₂O₄ nanosheet-mesoporous carbon composite electrode for enhanced reversible lithium storage. *Carbon* **2016**, 99, 633-641.
4. F. Fu, J. D. Li, Y. Z. Yao, X. P. Qin, Y. B. Dou, H. Y. Wang, J. K. Tsui, K. Y. Chan, M. H. Shao, Hierarchical NiCo₂O₄ Micro- and Nanostructures with Tunable Morphologies as Anode Materials for Lithium- and Sodium-Ion Batteries. *ACS Appl. Mater. Interfaces* **2017**, 9, 16194-16201.

5. H. Guo, L. X. Liu, T. T. Li, W. W. Chen, J. J. Liu, Y. Y. Guo, Y. C. Guo, Accurate hierarchical control of hollow crossed NiCo₂O₄ nanocubes for superior lithium storage. *Nanoscale* **2014**, *6*, 5491–5497.
6. H. S. Jadhav, R. S. Kalubarme, C. N. Park, J. Kim, C. J. Park, Facile and cost effective synthesis of mesoporous spinel NiCo₂O₄ as an anode for high lithium storage capacity. *Nanoscale* **2014**, *6*, 10071–10076.
7. S. Abouali, M. A. Garakani, Z. L. Xu, J. K. Kim, NiCo₂O₄/CNT nanocomposites as bi-functional electrodes for Li ion batteries and supercapacitors. *Carbon* **2016**, *102*, 262-272.
8. L. Peng, H. J. Zhang, Y. J. Bai, J. Yang, Y. Wang, Unique synthesis of mesoporous peapod-like NiCo₂O₄–C nanorods array as an enhanced anode for lithium ion batteries. *J. Mater. Chem. A* **2015**, *3*, 22094-22101.
9. Y. H. Wei, F. L. Yan, X. Tang, Y. Z. Luo, M. Zhang, W. F. Wei, L. B. Chen, Solvent-Controlled Synthesis of NiO-CoO/Carbon Fiber Nanobrushes with Different Densities and Their Excellent Properties for Lithium Ion Storage. *ACS Appl. Mater. Interfaces* **2015**, *7*, 21703-21711.
10. Y. P. Zhang, Q. Q. Zhuo, X. X. Lv, Y. Y. Ma, J. Zhong, X. H. Sun, NiO-Co₃O₄ nanoplate composite as efficient anode in Li-ion battery. *Electrochimica Acta* **2015**, *178*, 590-596.
11. Z. W. Zhang, Q. Li, Z. Q. Li, J. Y. Ma, C. X. Li, L. W. Yin, X. P. Gao, Partially Reducing Reaction Tailored Mesoporous 3D Carbon Coated NiCo-NiCoO₂/Carbon Xerogel Hybrids as Anode Materials for Lithium Ion Battery with Enhanced Electrochemical Performance. *Electrochimica Acta* **2016**, *203*, 117-127.
12. Y. F. Wang, L. J. Zhang, Simple synthesis of CoO–NiO–C anode materials for lithium-ion batteries and investigation on its electrochemical performance. *Journal of Power Sources* **2012**, *209*, 20-29.
13. X. N. Leng, Y. Shao, L. B. Wu, S. F. Wei, Z. H. Jiang, G. Y. Wang, Q. Jiang, J. S. Lian, A unique porous architecture built by ultrathin wrinkled NiCoO₂/rGO/NiCoO₂ sandwich nanosheets for pseudocapacitance and Li ion storage. *J. Mater. Chem. A* **2016**, *4*, 10304-10313.
14. D. Luo, Y. P. Deng, X. L. Wang, G. R. Li, J. Wu, J. Fu, W. Lei, R. L. Liang, Y. S. Liu, Y. L. Ding, A. P. Yu, Z. W. Chen, Tuning Shell Numbers of Transition Metal Oxide Hollow Microspheres toward Durable and Superior Lithium Storage. *ACS Nano* **2017**, *11*, 11521–11530.

Table S3. Electrochemical performance comparison of Co-Ni bimetal-oxide based supercapacitor electrodes. (PM: preparation method; SC: specific capacitance; RP: rate performance.)

| Ref. | Composite | PM | SC | RP |
|-----------|---|---|---|---------------------------------|
| This work | NiO@Co ₃ O ₄ @GQDs | Calcination and hydrothermal method | 1361 F g ⁻¹ (1 A g ⁻¹) | 55.3% (30 A g ⁻¹) |
| 1 | NiCo ₂ O ₄ -rGO | Hydrothermal method | 1185 F g ⁻¹ (2 A g ⁻¹) | 86.7% (8 A g ⁻¹) |
| 2 | Layered NiCo ₂ O ₄ /RGO | Electrostatic self-assembly | 1348 F g ⁻¹ (1 A g ⁻¹) | 62.3% (30 A g ⁻¹) |
| 3 | CKF/CoNiOx | Hydrothermal and calcination method | 711.1 F g ⁻¹ (1 A g ⁻¹) | 64.1% (2 A g ⁻¹) |
| 4 | NiCo ₂ O ₄ hollow micro-sphere | Hydrothermal method | 942.2 F g ⁻¹ (0.5 A g ⁻¹) | 75.5% (5 A g ⁻¹) |
| 5 | NiCo ₂ O ₄ hollow microspheres | Template method and thermal treatment | 720 F g ⁻¹ (2 A g ⁻¹) | 80.6% (25 A g ⁻¹) |
| 6 | Co ₃ O ₄ nanowire@NiO nanosheet arrays | Hydrothermal and electrodeposition method | 230.4 F g ⁻¹ (0.5 A g ⁻¹) | 59.3% (8 A g ⁻¹) |
| 7 | NiO@Co ₃ O ₄ nanowire arrays | Hydrothermal method | 1236.67 F g ⁻¹ (1 A g ⁻¹) | 67.7% (20 A g ⁻¹) |
| 8 | Rod-like nickel cobaltite/graphene | Hydrothermal method | 845 F g ⁻¹ (0.25 A g ⁻¹) | 33.3% (20 A g ⁻¹) |
| 9 | Hollow NiCo ₂ O ₄ nanowall arrays | Calcination method | 1055.3 F g ⁻¹ (2.5 mA cm ⁻²) | 45.8% (60 mA cm ⁻²) |
| 10 | NiCo ₂ O ₄ @MnO ₂ nanosheet networks | Electrodeposition method | 913.6 F g ⁻¹ (0.5 A g ⁻¹) | 55.2% (20 A g ⁻¹) |
| 11 | Nickel/cobalt oxide composite hollow spheres | Gasflow atomization and template method | 630 F g ⁻¹ (1 A g ⁻¹) | 54.3% (20 A g ⁻¹) |
| 12 | NiCo ₂ O ₄ -decorated porous carbon nanosheets | Hydrothermal method | 596.8 F g ⁻¹ (2 A g ⁻¹) | 26.8% (20 A g ⁻¹) |
| 13 | PPy-NiCo ₂ O ₄ | Hydrothermal and electrodeposition method | 910 F g ⁻¹ (1 A g ⁻¹) | 30.8% (5 A g ⁻¹) |
| 14 | NiCo ₂ O ₄ hollow spheres | Solvothermal and calcination method | 1141 F g ⁻¹ (1 A g ⁻¹) | 68.7% (15 A g ⁻¹) |

References:

1. S. Al-Rubaye, R. Rajagopalan, S. X. Dou and Z. X. Cheng, Facile synthesis of a reduced graphene oxide wrapped porous NiCo₂O₄ composite with superior performance as an electrode material for supercapacitors, *J. Mater. Chem. A*, 2017, 5, 18989-18997.
2. Q. Li, C. X. Lu, C. M. Chen, L. J. Xie, Y. D. Liu, Y. Li, Q. Q. Kong and H. Wang, Layered NiCo₂O₄/reduced graphene oxide composite as an advanced electrode for supercapacitor, *Energy Storage Mater.*, 2017, 8, 59-67.

3. W. B. Xu, B. Mu and A. Q. Wang, Three-dimensional hollow microtubular carbonized kapok fiber/cobalt-nickel binary oxide composites for high-performance electrode materials of supercapacitors, *Electrochim. Acta*, 2017, 224, 113-124.
4. C. C. Ji, F. Z. Liu, L. Xu and S. C. Yang, Urchin-like NiCo₂O₄ hollow microspheres and FeSe₂ micro-snowflakes for flexible solid-state asymmetric supercapacitors, *J. Mater. Chem. A*, 2017, 5, 5568-5576.
5. X. H. Qi, W. J. Zheng, G. H. He, T. F. Tian, N. X. Du and L. Wang, NiCo₂O₄ hollow microspheres with tunable numbers and thickness of shell for supercapacitors, *Chem. Eng. J.*, 2017, 309, 426-434.
6. D. D. Han, X. Y. Jing, J. Wang, Y. S. Ding, Z. Y. Cheng, H. Dang and P. C. Xu, Three-dimensional Co₃O₄ Nanowire@NiO Nanosheet Core-shell Construction Arrays as Electrodes for Low Charge Transfer Resistance, *Electrochim. Acta*, 2017, 241, 220-228.
7. Q. Q. Hu, Z. X. Gu, X. T. Zheng and X. J. Zhang, Three-dimensional NiO@Co₃O₄ hierarchical nanowire arrays for solid-state symmetric supercapacitor with enhanced electrochemical performances, *Chem. Eng. J.*, 2016, 304, 223-231.
8. Y. Lv, H. L. Wang, X. N. Xu, J. Shi, W. Liu and X. Wang, Balanced mesoporous nickle cobaltite-graphene and doped carbon electrodes for high-performance asymmetric supercapacitor, *Chem. Eng. J.*, 2017, 326, 401-410.
9. C. Guan, X. M. Liu, W. N. Ren, X. Li, C. W. Cheng and J. Wang, Rational Design of Metal-Organic Framework Derived Hollow NiCo₂O₄ Arrays for Flexible Supercapacitor and Electrocatalysis, *Adv. Energy Mater.* 2017, 1602391.
10. Y. B. Zhang, B. Wang, F. Liu, J. P. Cheng, X. W. Zhang and L. Zhang, Full synergistic contribution of electrodeposited three-dimensional NiCo₂O₄@MnO₂ nanosheet networks electrode for asymmetric supercapacitors, *Nano Energy*, 2016, 27, 627-637.
11. N. Wang, P. Zhao, Q. Zhang, M. Q. Yao and W. C. Hu, Monodisperse nickel/cobalt oxide composite hollow spheres with mesoporous shell for hybrid supercapacitor: A facile fabrication and excellent electrochemical performance, *Composites Part B*, 2017, 113, 144-151.
12. V. Veeramani, R. Madhu, S. M. Chen, M. Sivakumar, C. T. Hung, N. Miyamoto and S. B. Liu, NiCo₂O₄-decorated porous carbon nanosheets for high-performance supercapacitors, *Electrochim. Acta*, 2017, 247, 288-295.
13. T. H. Ko, D. Y. Lei, S. Balasubramaniam, M. K. Seo, Y. S. Chung, H. Y. Kim and B. S. Kim, Polypyrrole-Decorated Hierarchical NiCo₂O₄ Nanoneedles/Carbon Fiber Papers for Flexible High-Performance Supercapacitor Applications, *Electrochim. Acta*, 2017, 247, 524-534.
14. L. F. Shen, L. Yu, X. Y. Yu, X. G. Zhang and X. W. Lou, Self-templated formation of uniform NiCo₂O₄ hollow spheres with complex interior structures for lithium-ion batteries and supercapacitors. *Angew. Chem. Int. Ed.*, 2015, 54, 1868-1872.